JOURNAL OF Applied Polymer SCIENCE

Vacuum membrane distillation simulation of desalination using polypropylene hydrophobic microporous membrane

Na Tang,[1,2] Ying Peng,[1,2] Zhongyuan Jia,[1,2] Lei Zhang,[1,2] Jun Xiang,[1,2] Lina Yuan,[1,2] Penggao Cheng,[1,2] Xuekui Wang[1,2]

[1]College of Marine Science and Engineering, Tianjin University of Science and Technology, Tianjin 300457, China
[2]Tianjin Key Laboratory of Marine Resources and Chemistry, Tianjin 300457, China
Correspondence to: N. Tang (E-mail: tjtangna@tust.edu.cn)

ABSTRACT: Numerical simulation is an effective method to get the optimal operating parameters in the chemical engineering process. In this work, the transport mechanism of vacuum membrane distillation (VMD) process was simulated and predicted by mathematical model, which was established based on the convective heat transfer coefficient, and 0.5*M* aqueous NaCl solution was concentrated with isotactic polypropylene (iPP) hydrophobic microporous membrane prepared via thermally induced phase separation (TIPS) in the VMD process. The as-presented mathematical model simulated the effects of different operating parameters on the VMD performances for aqueous NaCl solution, such as feed temperature, feed flow rate, absolute pressure of membrane permeate side, temperature coefficient, membrane thickness, and porosity. A comparison between experimental data and simulated data was also considered to verify the proposed mathematical model. Additionally, the salt rejection of aqueous NaCl solution production water in VMD was higher than 99.9%. © 2014 Wiley Periodicals, Inc. J. Appl. Polym. Sci. **2015**, *132*, 41632.

KEYWORDS: copolymers; hydrophilic polymers; membranes; separation techniques

Received 9 May 2014; accepted 20 October 2014
DOI: 10.1002/app.41632

INTRODUCTION

Membrane distillation (MD) is a thermally driven process, in which only vapor molecules are transported through porous hydrophobic membranes.[1] The permeate side of the membrane may consist of a condensing fluid in direct contact with the membrane (DCMD),[2] a condensing surface separated from the membrane by an air gap membrane distillation (AGMD) a sweeping gas membrane distillation (SGMD), or a vacuum membrane distillation (VMD).[3,4] The type of MD employed is dependent upon permeate composition, flux, and volatility.[5–7] The porous membrane used in membrane distillation process is often made of hydrophobic material available in hollow fiber or flat-sheet forms such as polypropylene (PP),[8–11] poly(vinylidene fluoride) (PVDF),[12–14] and polytetrafluoroethylene (PTFE).[15] Compared with PVDF and PTFE, there are some advantages of isotactic polypropylene (iPP). It is an outstanding membrane material because of its low cost. Besides, it has good mechanical properties, high thermal stability, and excellent resistance to acids, alkalis, and organic solvent.[16] Thermally induced phase separation (TIPS), based on the dependence of the polymer solubility on the temperature, offers an attractive way to prepare iPP membrane because iPP can be dissolved in some solvents at about melting temperature of pure iPP.

The potential advantages of MD process in comparison with the conventional separation process rely on the lower operating temperature and hydrostatic pressure. Feed solutions having temperatures much more lower than its boiling point under pressures near atmosphere can be used. Benefiting from the above advantages, MD could be applied in many industrial processes, such as brine desalination,[17] waste water treatment,[18,19] food,[20] and energy industry.[21] Therefore, MD is now being investigated worldwide as a low-cost and energy-saving alternative to conventional separation processes such as conventional distillation and reverse osmosis.[22] VMD process received a great deal of attention by many investigators because of its promising applications in several separation areas. It is also a rising technology for seawater or brine desalination process. VMD process is based upon using a macroporous hydrophobic membrane for the separation of an aqueous feed solution and a downstream gaseous phase kept under vacuum. The driving

Additional Supporting Information may be found in the online version of this article.

force of the VMD is the partial pressure difference gradient across the membrane. Nonetheless, from a commercial standpoint, VMD is not implemented yet in industry for the main barrier of optimizing operating conditions.[23–26] Some researchers have already optimized the VMD process by numerical simulation. The heat and mass transfer processes were analyzed to build a mathematic model of cross-flow VMD process.[27,28] Besides, computational fluid dynamics (CFD) was employed to study the fluid dynamics of two-dimensional model for VMD a in our former study.[29] A two-dimensional geometry model of hollow fiber membrane was established by using the business software GAMBIT, and the flow conditions were set up using FLUENT software. Unfortunately, for a given hydrophobic microporous membrane, how to establish the mathematical model which describes the relationship between heat transfer and mass transfer correctly of aqueous NaCl solution in VMD process has not been reported as far as we know.

In this work, the numerical simulation of hollow fiber membrane module was modeled to describe the aqueous NaCl solution in VMD process. The relationship between heat transfer and mass transfer of aqueous NaCl solution in VMD process was investigated first. The membrane fibers in membrane module were narrow pore size distribution iPP membranes, which were prepared at optimum operating conditions via thermally induced phase separation (TIPS). The mathematical model of aqueous NaCl solution in the VMD process using the resultant membranes module was established, and the comparison of permeate flux between experimental data and mathematical simulated results was done to verify the model. The effects of feed temperature, feed flow rate, membrane permeates side pressure, membrane thickness, and membrane porosity on permeate flux and temperature polarization coefficient were investigated by simulation in the VMD process. This work would be helpful for the application of VMD and numerical simulation as well as technology design for desalination.

EXPERIMENTAL

Materials

Isotactic polypropylene (iPP) (melt index = 3.0 g/10 min, average molecular weight = 412,000) was supplied by Huabei Petrochemical Co.Ltd., China. Soybean oil (diluent) was purchased from Northsea Oils & Industries (Tianjin) Co. Ltd., China. Adipic acid (reagent purity) and hexane (reagent purity) were purchased from Tianjin Kemiou Chemical Reagent (China) and Tianjin Yingda Chemical Reagent (China), respectively. All chemicals were used without further purification.

Membrane Preparation

A casting solution was made up of about 27% (w/w) iPP, 73% (w/w) soybean oil (dilute), and 0.05% (w/w) adipic acid (nucleating agent). The mixed iPP hydrophobic microporous membranes for MD were prepared by TIPS, and the porosity was 60%. The thickness of the resulting membranes was 210 μm. And the maximum pore size of the membrane was 7 μm, respectively.[30,31]

Experimental Set-Up and Methods

A schematic view of the VMD experimental set-up was presented in Figure 1; 0.5*M* aqueous NaCl solution was continuously fed by a pump to the membrane module from a reservoir; the feed flow rate was controlled by a rotameter. When the feed was heated to the desired temperature, and a vacuum pump was connected to the permeate side of the membrane module to remove the water vapor flux. The vapor transferred through the membrane pores to the vacuum side and was collected in liquid nitrogen cold traps and was sampled every a certain time. The absolute pressure in the vacuum side was 3.0 kPa. The weight of permeation collected in the cold trap was measured continuously to calculate the VMD flux, *J*.

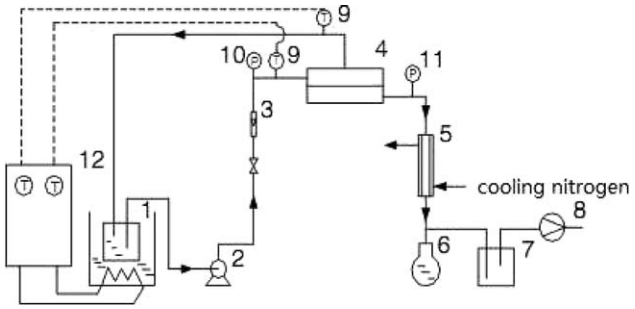

Figure 1. Schematic view of the VMD set-up. 1. Feed reservoir; 2. pump; 3. rotameter; 4. membrane module; 5. condensation tube; 6. flask for sampling; 7. buffer bottle; 8. waterpower vacuum pump; 9. thermometer; 10. manometer; 11. vacuum meter; 12. temperature controller.

$$J = \frac{W}{A \cdot t} \quad (1)$$

where J is the VMD flux, kg/(m^2 h), W is the weight of vapor across the membrane, kg; A is the effective membrane area, m^2, and t is the experimental running time, h.

Feed flux is the ratio of feed flow and membrane area.

$$F = \frac{Q}{A}. \quad (2)$$

In this equation, "F" means feed flux, kg/(m^2 h), "Q" means feed flow, kg/h, and "A" means membrane area (m^2).

η describes the salt rejection for the permeation selectivity of aqueous NaCl solution:

$$\eta = \frac{C_F - C_P}{C_F} \times 100\% \quad (3)$$

where, η is the salt rejection, %, C_F is the concentration of Cl^- in aqueous NaCl solution, *M*. $C_P$is the concentration of Cl^- in permeation solution, *M*.

VMD MATHEMATICAL MODELS

Transfer Mechanism for Aqueous NaCl Solution in VMD Process

The mechanism of transport in VMD involves simultaneously both heat transfer and mass transfer. Generally, the transport mechanism of VMD for aqueous NaCl solution can be summarized in the following steps: evaporation of water at the warm feed side of the membrane, migration of water vapor through the nonwetted pores, and condensation of water vapor transported outside of the permeate side of the membrane.[3,4] The main requirements of this process are that the membrane must not be wetted and only vapor is present in the pores.

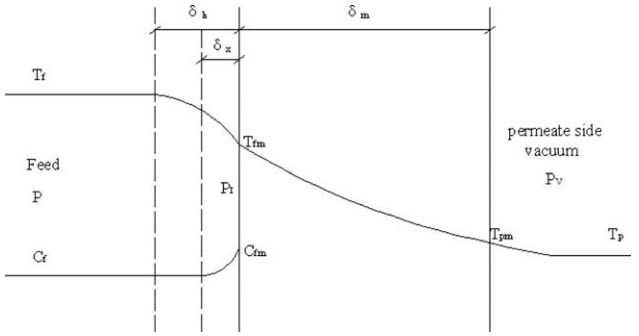

Figure 2. Diagram of heat and mass transfer of aqueous NaCl solution in VMD process. T_{fm}, T_{pm}, T_f, and T_p (K) are membrane interface temperatures and fluid bulk temperatures at the feed and permeate side, respectively. δ_h, δ_m, and δ_x (m) are the thicknesses of thermal boundary layer, membrane, and concentration boundary layer, respectively. P, P_f, and P_v (Pa) are pressures of the feed side, interfacial surface, and vacuum side, respectively. C_f and C_{fm} (M) are the concentration of nonvolatile solute(s) at the bulk feed and at the membrane surface, respectively.

A schematic drawing of the heat transfer and mass transfer mechanism in VMD process was shown in Figure 2. T_{fm}, T_{pm}, T_f, and T_p (K) were membrane interface temperatures and fluid bulk temperatures at the feed and permeate side, respectively. δ_h, δ_m, and δ_x (m) were the thicknesses of thermal boundary layer, membrane and concentration boundary layer, respectively. P, P_f, and P_v (Pa) were pressures of the feed side, interfacial surface, and vacuum side, respectively. C_f and C_{fm} (M) were the concentration of nonvolatile solute(s) at the bulk feed and at the membrane surface, respectively.

The driving force for water vapor migration through the membrane pores was the temperature difference between the feed/membrane interface temperature (T_{fm}) and permeate/membrane interface temperature (T_{pm}). Due to the heat losses in MD process, the membrane/interface temperatures were different from the bulk temperatures. This could be considered as one of the MD process drawbacks. This temperature difference led to a decrease from the theoretical driving force, which was defined as the difference between the bulk feed temperature (T_f) and the bulk permeate temperature (T_p). This phenomenon was known as temperature polarization.[3,4] The temperature polarization coefficient (TPC) was defined as the ratio between the actual driving force and the theoretical driving force, as a result, the temperature polarization coefficient was expressed mathematically as following:

$$TPC = \frac{T_{fm} - T_{pm}}{T_f - T_p} \tag{4}$$

where, T_{fm}, T_{pm}, T_f, and T_p were the same as before.

It was impossible to measure the membrane/interface temperatures experimentally. Usually, these temperatures were evaluated by performing a heat balance that relates them to the bulk temperatures. In order to solve this heat balance for membrane interface temperatures, the heat transfer coefficients in the adjoining liquid boundary layers to the membrane should be evaluated. Generally, the boundary layers heat transfer coefficients were evaluated using empirical correlations for the determination of Nusselt number, and a wide variety of these correlations were available in the literatures,[31,32] thus, facilitate the evaluation of the membrane surface temperatures. In the MD literatures, Dittus-Boelter correlation was often used to estimate the heat transfer coefficients. The formula was expressed mathematically as following:[31,32]

$$Nu = \frac{h_f d}{k^T} = 0.023 \mathrm{Re}^{0.8} \mathrm{Pr}^{1/3} \phi_u = 0.023 \left(\frac{du\rho}{\mu}\right)^{0.8} \left(\frac{c_P \mu}{k^T}\right)^{1/3} \left(\frac{\mu}{\mu_{\mathrm{wall}}}\right)^{0.14} \tag{5}$$

In VMD process, $\left(\frac{\mu}{\mu_{\mathrm{wall}}}\right)^{0.14}$ equaled to one, thus the formula could be written as:

$$Nu = \frac{h_f d}{k^T} = u Re^s Pr^t \tag{6}$$

where N_u was Nusselt number, R_e was Reynolds number, $R_e = \frac{du\rho}{\mu}$, P_r was Prandtl number, $P_r = \frac{C_p \mu}{K^T}$, d was the tube diameter, $\rho$was the fluid density, $\mu$was the bulk liquid viscosity, C_p was the liquid heat capacity, $K^T$was the thermal conductivity of the liquid, u, s, t were parameters in this equation.

Mass Transfer for Aqueous NaCl Solution in VMD Process

The hydrophobic VMD membrane is a porous medium. The mass transport mechanism in a porous medium was governed by three basic mechanisms known as Knudsen-diffusion (K), Poiseuille-flow (P), molecular–diffusion (M).[3,4] In detail, Knudsen diffusion is a diffusion that occurs when the scale length of a system is comparable to or smaller than the mean free path of the particles involved. Molecular diffusion is diffusion that molecular–molecular collision played an important role, which is suitable for the condition that the scale length of a system is much larger than the particles. The Knudsen number (K_n):

$$\mathrm{K_n} = \frac{1}{\mathrm{d}} \tag{7}$$

It is used to judge the dominating mechanism of the mass transfer in the pores. Here, l is the mean free path of the transferred gas molecules and d is the mean pore diameter of the membrane. Table I shows the dominating mass transfer mechanism based on K_n in a gas mixture with a uniform pressure throughout the system.[33] As the pore size of the VMD membranes is in general in the range of 0.2 to 1.0 μm (pore diameter was 0.3–0.6 μm in our membrane) and the mean free path of the water vapor is 0.63 μm at 0.5 KPa and 60°C in VMD process (Comparing with water vapor is 0.11 μm at 0.1 MPa and 60°C in MD process). K_n calculated from eq. (7) is in the range of 2.10 to 1.05. In VMD the downstream pressure is reduced below the equilibrium vapor pressure, so that a convective transport mechanism is dominant for mass transfer. In view of the low pressure values prevailing in the gaseous phase, the molecular mean free path of the water vapor is substantially

Table I. Mass Transfer Mechanism in Membrane Pore

Molecular diffusion	Knudsen-molecular diffusion transition mechanism	Knudsen mechanism
$K_n < 0.01$	$0.01 < K_n < 1$	$K_n > 1$

Table II. The Parameters of the Self-Made Membranes

P_v (Pa)	R (J/(mol K))	π	M_{H_2O}(kg/mol)	ε (%)	R (m)
3000	8.314	3.1416	0.018	60	4×10^{-8}
δ (m)	τ	v (m/s)	c_p (J/(kg K))	a (m)	b (m)
2.1×10^{-4}	1.4	20	4181	3.4×10^{-3}	3.3×10^{-3}

Parameters "v", "a," and "b" means the average movement speed of vapor molecular, the long, and length of cross-section of the flow channel, respectively.

larger than the pore sizes of the membranes typically used in MD processes. As a consequence, mass transfer through the membrane is generally dominated by Knudsen diffusion mechanism, and molecular diffusion is neglected. Poiseuille flow is pressure-induced flow in a long duct, usually a pipe. In this work, the pore diameter and the pore length is 0.3to 0.7 μm and 100 to 250 μm, respectively. As a result, the combination of Knudsen diffusion and Poiseuille diffusion was employed in this work. The mass transfer flux across the membrane of aqueous NaCl solution could be obtained by calculating the following equations:

$$N_i=\frac{1}{RT_{\text{avg}}\delta}\left[K_0\left(\frac{8\text{RT}_{\text{avg}}}{\pi M_i}\right)^{1/2}\Delta P_i+B_0\frac{P_{\text{iavg}}}{\mu_g}\Delta P\right] \quad (8)$$

$$\Delta P_i=P_{\text{fm}_i}-P_{V_i} \quad (9)$$

where, N_i was the mass transfer flux across the membrane, $\triangle P_i$ and $\triangle P$ were the difference of vapor subpressure and total pressure on both sides of the membrane, respectively. P_{iavg} and T_{avg} were the mean pressure and temperature on both sides of the membrane, respectively. M_i was molar mass of the pure i substrate; μ_g was gas viscosity; δ was the membrane thickness; R was the universal gas constant (8.314 J/(mol K)); K_0 and B_0 were constants depended on the geometrical parameters of the membrane, which could be measured by gas permeate experiments or be given by the following equations.

$$B_0=\frac{\varepsilon r^2}{8\tau} \quad (10)$$

$$K_0=\frac{2\varepsilon r}{3\tau} \quad (11)$$

$$\Delta P=P_{\text{fm}}-P_V \quad (12)$$

where, ε was membrane porosity, τ was Bending factor of the membrane pore, and r was radius of the pores (m). P_{fm} and P_v were pressures of water vapor at the interfacial surface and membrane permeate side, respectively. The driving force of mass transfer flux across the membrane was the vapor pressure difference on both sides of the membrane. Vapor pressure on vapor-liquid interface, P_{fm} was affected by the concentration of aqueous NaCl solution, which could be calculated by formula (13).[34–36]

$$P_{\text{fm}_i}=x_i\gamma_{\text{water}}P_i^0 \quad (13)$$

$$P_i^0=\exp\left[23.1964-\frac{3816.44}{T_{\text{fm}}-46.13}\right] \quad (14)$$

$$T_{\text{Pm}}=\frac{3816.44}{23.1964-\ln P_V}+46.13 \quad (15)$$

where, P_i^0 was the saturated water vapor pressure on vapor-liquid interface, which could be calculated by Antoine equation. x_i was the molar ratio of water in the bulk, and γ_{water} was the activity coefficient of water in aqueous NaCl solution.

In the experiment, x_{water} equaled to 0.99108.[37] Water activity coefficient γ_{water} could be estimated by NRTL equation, UNIQUAC equation, Wilson equation, or Van Laar equation, etc. and Van Laar equation and NRTL equation were better applied to different MD models.[38–40] Schofield had proved that the water activity coefficient of aqueous NaCl solution could be solved by the following formula:[41]

$$\gamma_{\text{water}}=1-0.5x_{\text{NaCl}}-10x_{\text{NaCl}}^2 \quad (16)$$

where, χ_{NaCl} was the molar ratio of NaCl in the bulk of the feed. In this work, χ_{NaCl} equaled to 0.00892, thus γ_{water} was 0.99474.

The formulas used in aqueous NaCl solution mathematical model for VMD process were summed up and listed in the Appendix.

The software Matlab was used in this work. The parameters of the self-made membranes were listed in the Table II.

In order to simplify the simulation, the regressed u, s, t was used to replace the u, s, t coefficients in Dittus-Boelter correlation. The process of computing correlation coefficients u, s, and t were regressed in Figure 3.

RESULTS AND DISCUSSION

Effect of Feed Temperature and Feed Flow Rate

Effect of Feed Temperature and Feed Flow Rate on VMD Permeate Flux. The effect of feed temperature and feed flow rate was shown in Figure 4(a). The experiment was carried out at vacuum side absolute pressure of 3 kPa. Figure 4(a) showed that VMD flux increased with the increasing of feed temperature, however, VMD flux had minor change with feed flow rate increasing (the variance analysis was in Supporting Information Table S1–S3). The VMD flux increases with increasing feed temperature could be explained as follows. Increasing the feed temperature made the upside vapor pressure higher, leading to an increase of the mass transfer driving force, despite the fact that the downside vacuum degree was kept constant. In addition, the liquid viscosity was reduced by the temperature rising, and the improved fluidity of the feed enhances turbulent movement. The lower concentration polarization led to a decrease in mass transfer resistance. As the feed flow rate increases, the thickness of heat and mass transfer boundary layer on feed side became thinner, which reduced the resistance of heat transfer and mass transfer. However, the main resistance of heat transfer and mass transfer was the transmembrane resistance, and the feed flow rate played a trivial role on VMD flux.

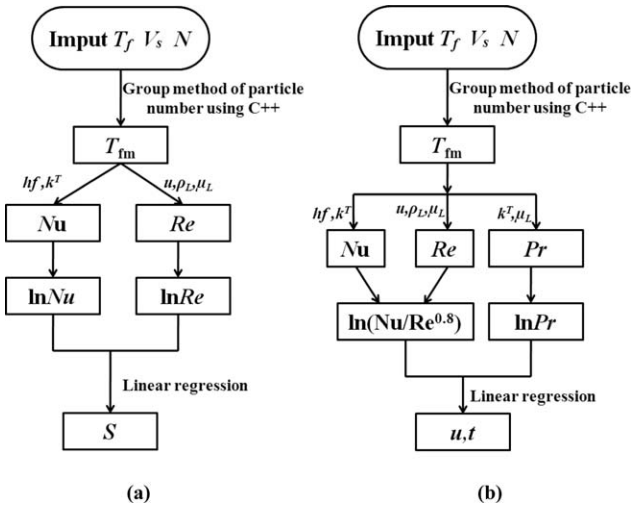

Figure 3. (a) The process computing parameters "s" with language C++. (b) The process computing parameters "u, t" with language C++.

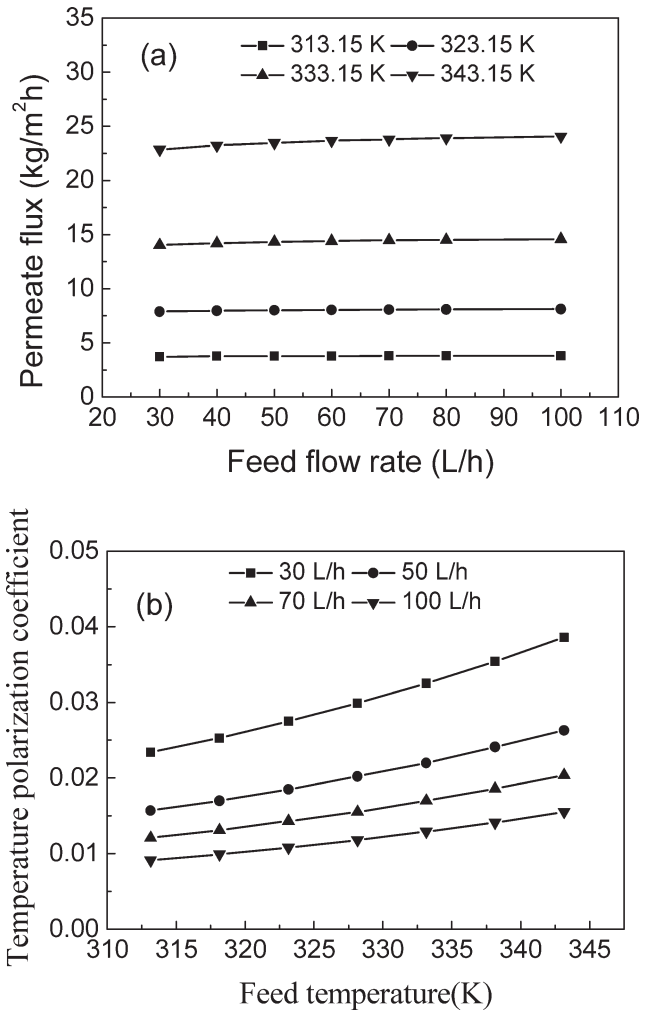

Figure 4. (a) Effect of feed temperature and rate on simulated permeate flux of aqueous. (b) Effect of feed temperature on simulated temperature polarization coefficient of aqueous NaCl solution for VMD.

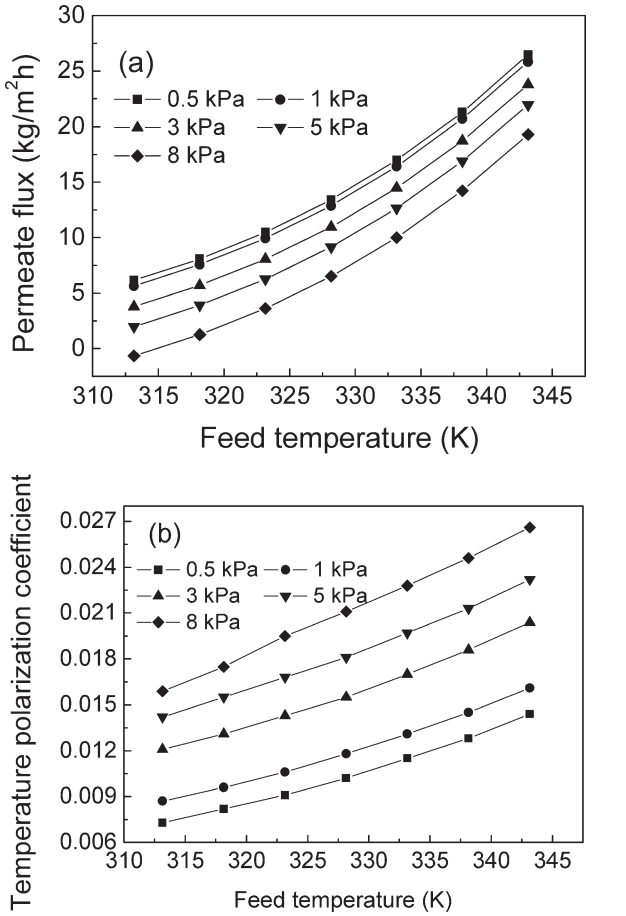

Figure 5. (a) Effect of membrane permeate side pressure on simulated permeate flux of aqueous NaCl solution for VMD. (b) Effect of membrane permeate side pressure on simulated temperature polarization coefficient of aqueous NaCl solution for VMD.

Effect of Feed Temperature and Feed Flow Rate on Temperature Polarization Coefficient. The simulated influence of feed temperature and feed flow rate on temperature polarization coefficient was shown in Figure 4(b) (the absolute pressure on vacuum side was kept at 3 kPa). It showed that the temperature polarization coefficient increased with the increasing of feed temperature at the same feed flow rate. Because the higher feed temperature caused a larger temperature dropping of heat boundary layer on vapor–liquid interface, which would result in the temperature polarization phenomenon. Additionally, the temperature polarization coefficient dropped obviously with the increasing of feed flow rate when the feed temperature was fixed. Due to the fact that feed flow rate increased, the resistance of heat transfer and mass transfer was reduced and the temperature decreases accordingly, which led to a decrease in the temperature polarization effect and temperature polarization coefficient in the VMD process.

Effect of Membrane Permeate Side Pressure

Effect of Membrane Permeate Side Pressure on VMD Permeate Flux. The effect of membrane permeate side pressure on permeate flux simulated by using mathematical method was shown in Figure 5(a). The permeate flux of aqueous NaCl solution

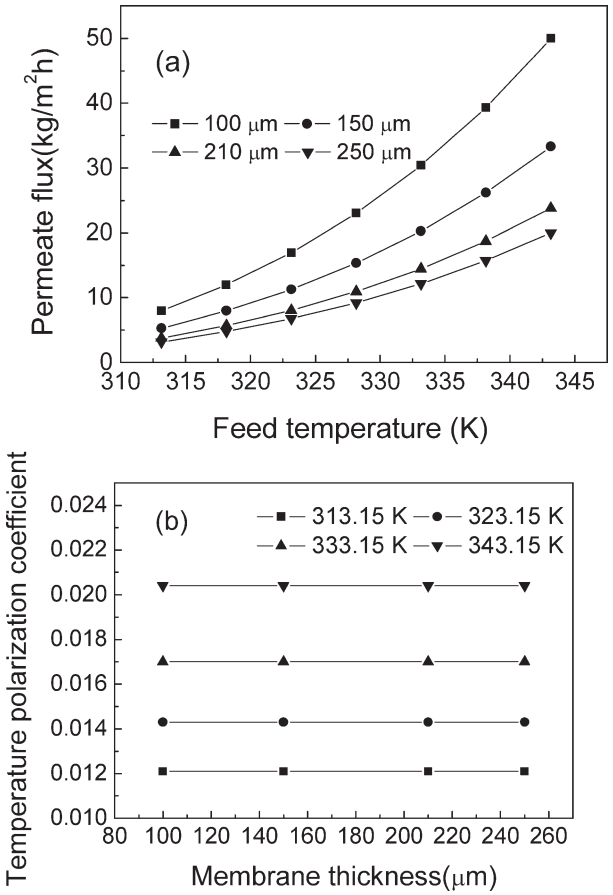

Figure 6. (a) Effect of membrane thickness on simulated permeate flux of aqueous NaCl solution for VMD. (b) Effect of membrane thickness on simulated temperature polarization coefficient of aqueous NaCl solution for VMD.

decreased obviously with increasing of the membrane permeate side pressure (the variance analysis was in Supporting Information Table S4). When feed flow rate and the saturated water vapor pressure were constants, membrane permeate side pressure had a negative effect on the driving force of mass transfer across the membrane, which reduced the permeate flux of aqueous NaCl solution for VMD. As shown in Figure 5(a), the mass transfer process could not be carried on when the feed temperature was 313.15 K and the pressure at membrane permeate side was 8 kPa.

Effect of Membrane Permeate Side Pressure on Temperature Polarization Coefficient. The effects of membrane permeate side pressure on temperature polarization coefficients were shown in Figure 5(b). The temperature polarization coefficients of aqueous NaCl solution increased with the increase of permeate side pressure, accordingly. The saturated water vapor temperature was increased with the increasing of permeate side pressure, and the temperature polarization phenomenon became more obvious at the same time.

Effect of Membrane Thickness

The membrane thicknesses were related with mass transfer rate and membrane mechanical stability, which mainly depends on spin speed and slit thickness. In this part, we explored the role of membrane thickness as a factor influencing permeate flux and temperature polarization coefficient. Figure 6(a) showed the effect of membrane thickness on flux when the absolute pressure on membrane permeates side was kept at 3 kPa. The permeate flux increased with the decreasing of the membrane thickness for smaller vapor resistance (the variance analysis was in Supporting Information Table S5). The effect of membrane thickness on the temperature polarization phenomenon simulated by using mathematical method was shown in Figure 6(b). As a result, the membrane thickness had negligible influence on the temperature polarization coefficient of aqueous NaCl solution in VMD.

Effect of Membrane Porosity on VMD Permeate Flux and Temperature Polarization Coefficient

The membrane porosity is a key factor correlated with membrane performance, which could be tuned by polymer concentration, quench temperature, and nucleating agent concentration during the process of membrane preparation. Thus, the membrane porosity on VMD permeate flux was investigated as shown in Figure 7(a). It was clearly showed that under the same feed condition, the permeate flux increased with the increasing of membrane porosity (the variance analysis was in Supporting

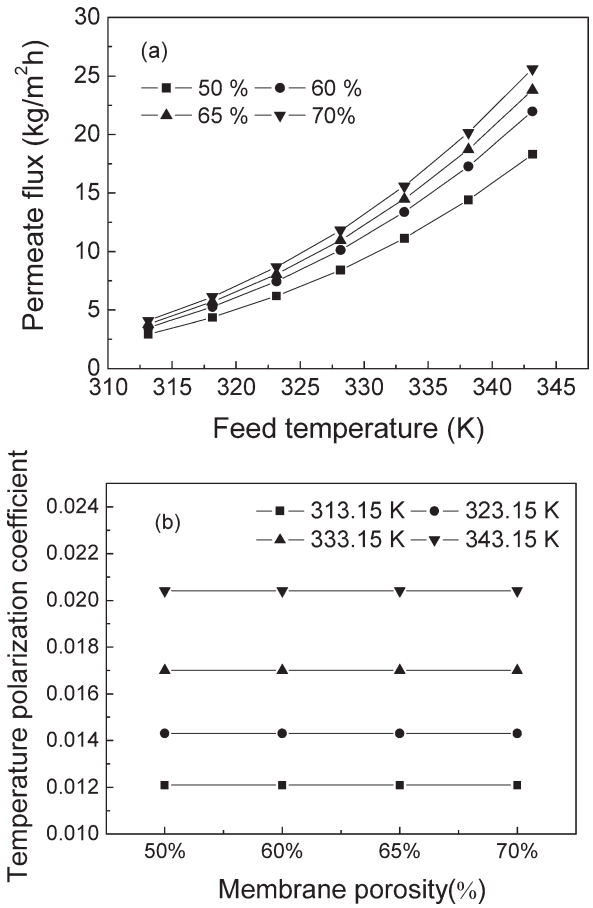

Figure 7. (a) Effect of membrane porosity on simulated permeate flux of aqueous NaCl solution for VMD. (b) Effect of membrane porosity on simulated temperature polarization coefficient of aqueous NaCl solution for VMD.

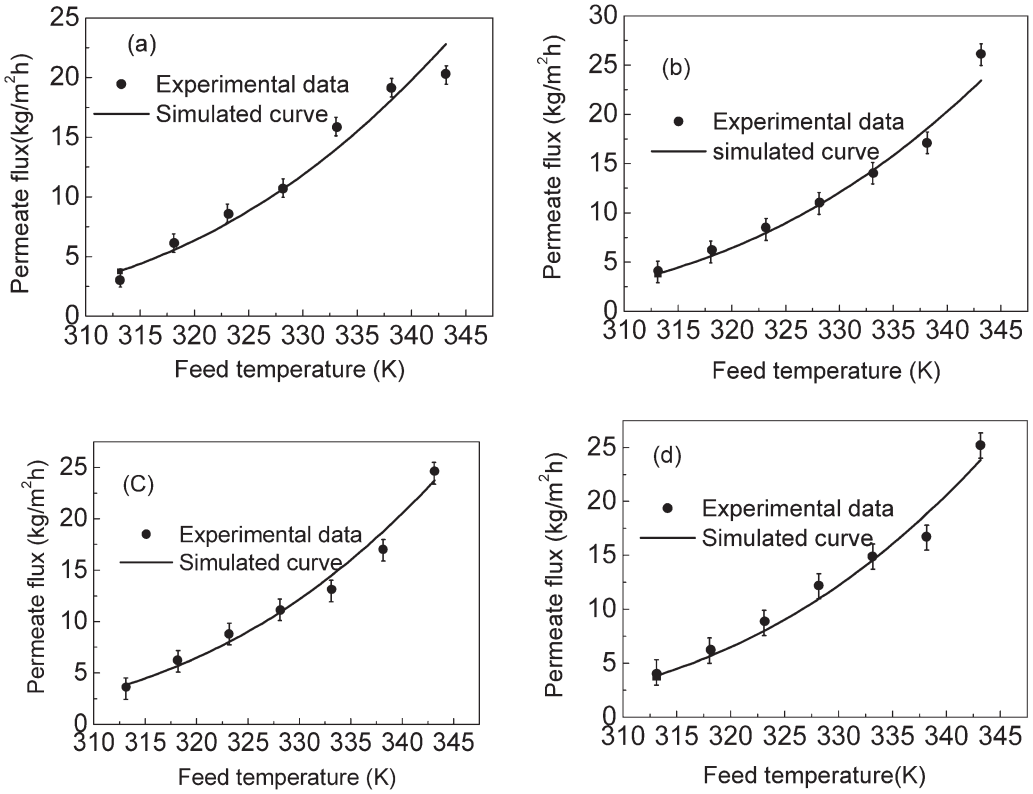

Figure 8. Comparison of experimental and simulated permeate flux for aqueous NaCl solution VMD with (a) feed flux 30 kg/(m^2 h), (b) feed flux 50 kg/(m^2 h), (c) feed flux 70 kg/(m^2 h), (d) feed flux 80 kg/(m^2 h).

Information Table S6). Membranes with higher porosity exhibited greater surface area for evaporation in the process of mass transfer crossing the membrane, which reduced the mass transfer resistance and increases the mass transfer flux. Especially, the improving membrane porosity was more helpful for enhancing flux under relatively higher temperature. In contrast, as shown in Figure 7(b), the effect of membrane porosity on flux was negligible. We postulated that the flux was determined by temperature and limited by porosity. More specifically, temperature determined mass transfer rate and porosity determined mass transfer resistance directly.

Table III. The Determination Results of Salt Rejection for Aqueous NaCl Solution VMD

No.	Cl^- concentration in aqueous NaCl solution(mg/L)	Cl^- concentration in production water (mg/L)	Desalinization ratio (%)
1	17,750	17.2	99.90
2	17,552	16.8	99.90
3	17,750	18.3	99.90
4	17,753	13.2	99.93
5	17,749	17.5	99.90
6	17,751	18.9	99.90
7	17,750	15.4	99.91
8	17,750	18.6	99.90
9	17,752	12.5	99.93
10	17,753	17.6	99.90

COMPARISON BETWEEN EXPERIMENTAL DATA AND MATHEMATICAL SIMULATED RESULTS FOR AQUEOUS NACL SOLUTION IN THE VMD PROCESS

Finally, comparisons of experimental and simulated permeate flux for aqueous NaCl solution VMD with a serial of feed fluxes were taken to validate the applicability of mathematical model for VMD process of aqueous NaCl solution. The experimental and simulated condition were both determined as 3 kPa (membrane permeates side absolute pressure) and 0.5*M* aqueous NaCl solution. As shown in Figure 8, the permeate flux of simulated results were agreed well with the experimental data under feed flux from 30 to 80 kg/(m^2 h). It could be concluded that as-established mathematical model could be used in the VMD process of aqueous NaCl solution. Moreover, salt rejection was investigated by measuring the concentration of chloride in aqueous NaCl solution and in production water during VMD process. As demonstrated in Table III, the salt rejection of production water was all up to 99.9%, which indicated that the self-prepared membrane was of excellent separation behavior.

CONCLUSIONS

The mathematical model of aqueous NaCl solution in the VMD process using self-made polypropylene hydrophobic membrane was established on the base of Knudsen-diffusion and Poiseuille-flow mechanism by the software of C++ language. Dittus-Boelter

correlation was employed to study the effects of the feed solution temperature, feed flow rate, membranes permeate side pressure, membrane thickness, and porosity on permeate flux and temperature polarization coefficient. Comparisons of experimental and simulated permeate flux for aqueous NaCl solution VMD with a serial of feed fluxes were taken to validate the applicability of mathematical model for VMD process of aqueous NaCl solution, which also could be used in desalination process by VMD. The temperature polarization coefficient decreased with the increasing of the feed flow rate, however, the feed flow rate played a trivial role on VMD flux. The increasing temperature of feed solution resulted in the increasing of permeate flux and temperature polarization coefficient. When the membrane permeate side pressure increased, the permeate flux decreased significantly and temperature polarization coefficient increased at the same time. Meanwhile the permeate flux increased with the increasing of membrane porosity and decreasing of membrane thickness. From the variance analysis results, it was shown that the temperature was first important factor, and the membrane thickness was the second important factor, the permeate side pressure was the third important factor, then the membrane porosity was forth important factor, and feed flow rate was the least important factor. In this work, all the desalination rates of production water via a VMD process were all above 99.9%.

ACKNOWLEDGMENTS

The authors thank for the financial support of National Nature Science Foundation (21376178), TIDA giant growth plan (2011-XJR13020), Tianjin Science and technology support program (12ZCDZSF06900), National Nature Science Foundation (12JCZDJC30000). The Training Program for Changjiang Scholars and Innovative Research Team in University ([2013]373) and the Innovative Research Team of Tianjin Municipral Education Commission (TD12-5004).

NOMENCLATURE

A	Effective membrane area, m^2.
C_F	Concentration of Cl^- in aqueous NaCl solution, *M*.
C_P	Concentration of Cl^- in permeation solution, *M*.
C_f	The concentration of nonvolatile solute(s) at the bulk feed, *M*.
C_{fm}	The concentration of nonvolatile solute(s) at the membrane surface, *M*.
C_p	The liquid heat capacity, *M*.
D	The tube diameter, m.
K^T	The thermal conductivity of the liquid.
J	VMD flux, kg/(m^2 h).
M_i	Molar mass of the pure *i* substrate.
N_u	Nusselt number.
N_i	The mass transfer flux across the membrane.
P	Pressures of the feed side, Pa.
P_I	Pressures of the interfacial surface, Pa.
P_v	Pressures of the vacuum side, Pa.
P_{fm}	Pressures of water vapor at the interfacial surface, Pa.
P_v	Pressures of water vapor at membrane permeate side, Pa.
P_i^0	Saturated water vapor pressure on vapor-liquid interface.
P_{iavg}	The mean pressure on both sides of the membrane, Pa.
P_r	Prandtl number.
$\triangle P_i$	The difference of vapor sub-pressure of the membrane, Pa.
$\triangle P$	The difference of total pressure on both sides, Pa.
R	Radius of the pores, m.
R_e	Reynolds number.
t	Experimental running time, h.
T_{fm}	Membrane interface temperatures at the feed side, K.
T_{pm}	Membrane interface temperatures at the permeate side, K.
T_f	Fluid bulk temperatures at the feed side, K.
T_p	Fluid bulk temperatures at the permeate side, K.
T_{avg}	The mean temperature on both sides of the membrane, K.
W	Weight of vapor across the membrane, kg.
x_i	Molar ratio of water in the bulk.
ρ	The fluid density.
μ	The bulk liquid viscosity.
μ_g	Gas viscosity.
η	Salt rejection, %.
δ_h	Thicknesses of thermal boundary layer.
δ_m	Thicknesses of membrane.
δ_x	Thicknesses of concentration boundary layer.
δ	The membrane thickness.
ε	Membrane porosity.
τ	Bending factor of the membrane pore.
γ_{water}	Activity coefficient of water in aqueous NaCl solution.

REFERENCES

1. Nghiem, L. D.; Hildinger, F.; Hai, F. I.; Cath, T. *Desalin. Water Treat.* **2011**, *32*, 234.
2. Hawlader, M. N. A.; Bahar, R.; Ng, K. C.; Stanley, L. J. W. *Desalin. Water Treat.* **2012**, *42*, 333.
3. Lawson, K. W.; Lloyd, D. R. *J. Membr. Sci.* **2007**, *124*, 1.
4. El-Bourawi, M. S.; Ding, Z.; Ma, R.; Khayet, M. *J. Membr. Sci.* **2006**, *285*, 4.
5. El-Fray, M.; Gryta, M. *Polimery* **2008**, *53*, 11.
6. Gryta, M. *J. Membr. Sci.* **2007**, *287*, 67.
7. Li, J. M.; Xu, Z. K.; Liu, Z. M.; Yuan, W. F.; Xiang, H.; Wang, S. Y.; Xu, Y. Y. *Desalination* **2003**, *155*, 153.
8. Tomaszewska, M. *Desalination* **1996**, *104*, 1.
9. Edwie, F.; Teoh, M. M.; Chung, T. S. *Chem. Eng. Sci.* **2012**, *68*, 567.
10. Teoh, M. M.; Chung, T. S.; Yeo, Y. S. *Chem. Eng. Sci.* **2011**, *171*, 684.
11. Akbari, A.; Hamadanian, M.; Jabbari, V.; Lehi, A. Y.; Bojaran, M. *Desalin. Water Treat.* **2012**, *46*, 96.
12. Hwang, H. J.; He, K.; Gray, S.; Zhang, J. H.; Moon, I. S. *J. Membr. Sci.* **2011**, *371*, 90.
13. Lai, C. L.; Liou, R. M.; Chen, S. H.; Huang, G. W.; Lee, K. R. *Desalination* **2011**, *267*, 184.
14. Lawson, K. W.; Lloyd, D. R. *J. Membr. Sci.* **1996**, *120*, 111.
15. Yang, Z. S.; Li, P. L.; Xie, L. X.; Wang, Z.; Wang, S. C. *Desalination* **2006**, *192*, 168.

16. Yang, Z. S.; Li, P. L.; Chang, H. Y. *Chin. J. Chem. Eng.* **2006**, *14*, 394.
17. Chen, H. Y.; Wu, C. R.; Jia, Y.; Wang, X.; Lu, X. L. *Desalin. Water Treat.* **2011**, *28*, 321.
18. Lu, Y. Y.; Chen, J. *Ind. Eng. Chem. Res.* **2011**, *50*, 7345.
19. Yarlagadda, S.; Gude, V. G.; Camacho, L. M. *J. Hazard. Mater.* **2011**, *192*, 1388.
20. Bagger-Jorgensen, R.; Meyer, A. S.; Pinelo, M.; Varming, C.; Jonsson, G. *Innov. Food Sci. Emerg.* **2011**, *12*, 388.
21. Lewandowicz, G.; Bialas, W.; Marczewski, B.; Szymanowska, D. *J. Membr. Sci.* **2011**, *375*, 212.
22. Schofield, R. W.; Fane, A. G.; Fell, C. J. D. *J. Membr. Sci.* **1987**, *33*, 299.
23. Yu, H.; Yang, X.; Wang, R.; Fane, A. G. *J. Membr. Sci.* **2011**, *384*, 107.
24. Khayet, M. *Adv. Colloid. Interface* **2010**, *164*, 56.
25. Cipollina, A.; Micale, G.; Rizzuti, L. *Desalin. Water Treat.* **2011**, *25*, 195.
26. Charfi, K.; Khayet, M.; Safi, M. J. *Desalination* **2010**, *259*, 84.
27. Wang, H. T.; Li, B. A.; Wang, L.; Song, S. S.; Wang, J. X.; Feng, Y. K.; Wang, S. C. *Ind. Eng. Chem. Res.* **2012**, *51*, 487.
28. Qi, B. W.; Li, B. A.; Wang, S. C. *Ind. Eng. Chem. Res.* **2012**, *51*, 11463.
29. Tang, N.; Zhang, H.; Wang, W. *Desalination* **2011**, *274*, 120.
30. Tang, N.; Jia, Q.; Zhang, H. J.; Li, J. J.; Cao, S. *Desalination* **2010**, *256*, 27.
31. Qtaishat, M. R. Use of Vacuum Membrane Distillation for Concentrating Sugars and Dyes from their Aqueous Solutions; M.Sc. Thesis. Jordan University of Science and Technology: Jordan, **2004**.
32. Holman, J. P. Heat Transfer; McGraw-Hill: New York, **1989**.
33. Bandini, S.; Saavedra, A.; Sarti, G. C. *J. AIChE* **1997**, *43*, 398.
34. Bandini, S.; Sarti, G. C. *J. AIChE* **1999**, *45*, 1422.
35. Ding, Z.; Ma, R.; Fane, A. G. *Desalination* **2003**, *151*, 217.
36. Lawson, K. W.; Lloyd, D. R. *J. Membr. Sci.***1997**, *124*, 1.
37. Sarti, G. C.; Gostoli, C.; Bandini, S. *J. Membr. Sci.* **1993**, *80*, 21.
38. Gostoli, C.; Sarti, G. C. *J. Membr. Sci.* **1989**, *33*, 211.
39. Saavedra, A.; Bandini, S.; Sarti, G. C. In Proceedings of the Euromembrane Conference; Paris, France, **1992**; p 119.
40. Izquierdo-Gil, M. A.; Abildskov, J.; Jonsson, G. *J. Membr. Sci.* **2004**, *239*, 227.
41. Martínez-Diez, L.; Vázquez-González, M. I. *J. Membr. Sci.* **2000**, *173*, 225.